Polymers for Near-field Electrospinning with Spatial Control

Antonio Osamu Katagiri Tanaka, Héctor Alán Aguirre Soto

Abstract

Near-field electrospinning (NFES) is identified to be a technique able to fabricate polymer nano and micro fibers with accurate placement. In the past years (2006-2019), several polymer solutions have been successfully electrospun into fibers through several variants of the conventional NFES process. Each NFES variant intents to tailor the process parameters in order to improve the fibers' properties. This paper presents a review on the research and related development of electrospun fibers, emphasizing the used polymers, solvents, and fiber characteristics. Relevant summary of polymer solutions and near-field electrospinning processing conditions is provided in this paper.

Keywords: polymer, solvent, near-field electrospinning, NFES, fibers, spatial control

Contents

Email addresses: oskatagiri@gmail.com (Antonio Osamu Katagiri Tanaka), alan.aguirre@tec.mx (Héctor Alán Aguirre Soto)

1. Types of electrospinning (Classified by process properties)

Even though electrospinning is an old invention [1], it is currently a trending topic among researchers [2–4]. One of the reasons electrospinning is to be studied is its potential to fabricate polymer nano fibers from a variety of polymers. The technique allows the production of thin continuous fibers with ease, with diameters down to 3 nm in some cases, which is something difficult to achieve by other techniques. Furthermore, the basic setup can be modified with ease to fabricate different fibers with diversified functionalities with different materials. The produced fibers can be aligned or unaligned. Besides, the electrospinning equipment is inexpensive and of small size, compared to the equipment of standard spinning techniques [5]. On the other hand, the understanding of the electrospinning process has improved in the last years.

Current literature dictates the typical spinning setup is comprised by three main components: a syringe needle, a fiber collector, and some way to dispense the fibers from the needle to the collector. The spinning process is an electrohydrodynamic (EHD) technique that yields continuous polymer fibers. Other EHD techniques are spraying and atomization which produce polymer droplets and polymer particles respectively.

In electrospinning the fibers are deposited by an electrical potential difference between the syringe needle and the collector. The supplied polymer (typically a polymer solution) is administrated at a constant rate to create and maintain a polymer drop at the dispensing nozzle. A high voltage (usually DC) is applied between the polymer feed and the collector. As the electric field increases, the polymer drop (held by its surface tension) is then deformed at the tip of the syringe needle to form a conical shape known as Taylor cone. When the electric force overcomes the surface tension force a polymer jet is ejected from the tip of the Taylor cone. As the polymer jet leaves the nozzle, it accelerates and stretches while traveling to the fiber collector. The fiber finally develops with the complete solvent evaporation.

1.1. High voltage power supply: Direct Current & Alternating Current

Direct current (DC) is typically used in electrospinning with the electrons flowing in one direction. Alternate current (AC) implementations are also studied as the AC creates a change in the direction of the current flow. Kessick et al. [6] demonstrated the implementation of AC power supplies in the production of polymer fibers.

The AC electrospinning setup is similar to that for the DC variant. AC electrospinning apparatus do not require a grounded collector as the current alternates. In AC, the produced fibers are prone to carry an electric charge, while those generated shortly after have an opposite charge. The difference in charges lead the fibers to discharge on each other, creating an aerogel plume of fibers. The optimal AC frequency depends on the materials used and is typically within of 50 Hz – 1 kHz. [7]

The AC technique has been studied for drug loaded related applications. Balogh et al. [8] compared fibers fabricated by DC and AC spinning techniques. They produced fibers by using three polymers: Eudragit EPO (cationic copolymer), Eudragit L100-55 (anionic polymer) and poly(vinyl pyrrolidone) (PVP) (neutral polymer). Balogh et al. discovered AC and DC electrospinning can produce fibers with all three polymers. However, The AC process allowed the implementation of faster flow rates than in the DC setup. The DC electrospinning technique generated fibers with a maximum flow rate of 5 ml/h; on the other hand, the AC setup allowed an increase in flow rate up to 40 ml/h. AC electrospinning approach is as effective as the DC technique

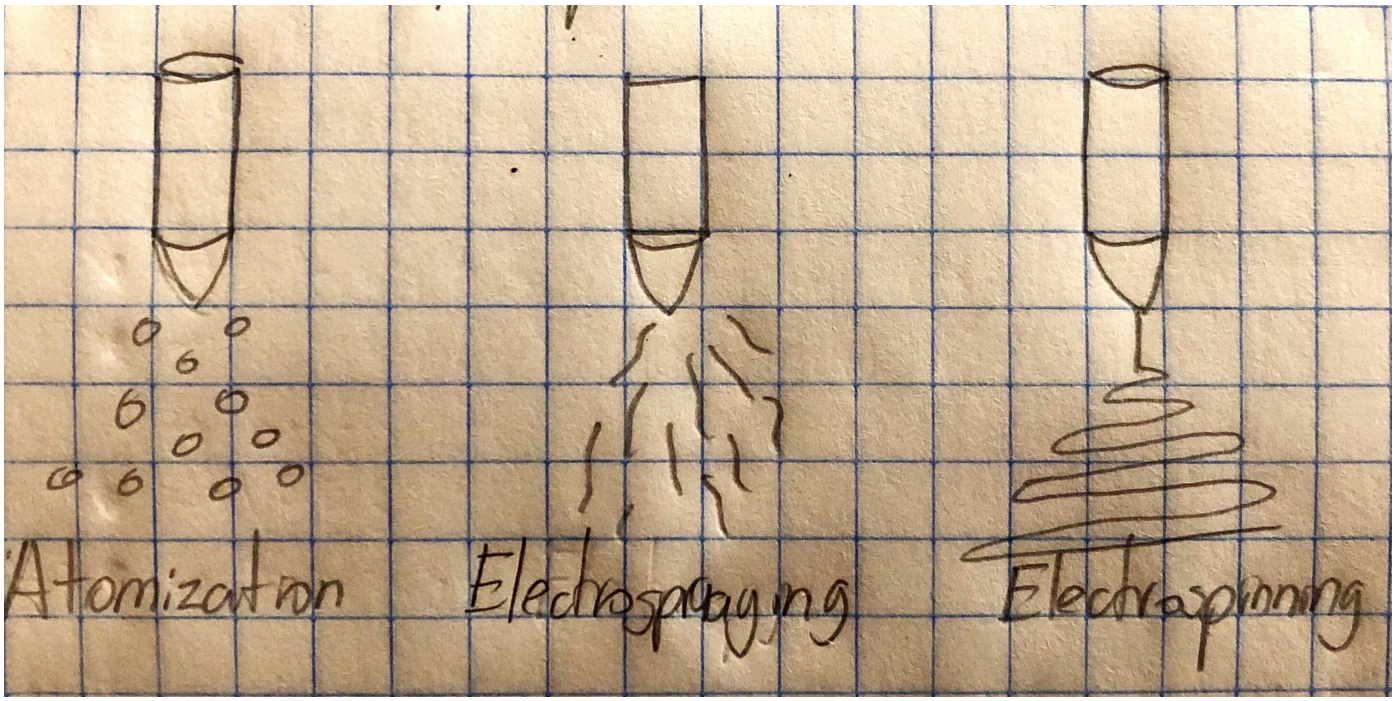

Figure 1: Electrohydro-dynamic techniques

in producing drug delivery systems.

1.2. Polymer reservoir: Polymer melt & Polymer solution

Another electrospinning classification is the melt process. As Brown et al. [9] discussed, the polymer melt is equivalent to the polymer solution electrospinning (in place of a polymer solution a melt is used). The use of a polymer melt increases the complexity of the process, because the nozzle syringe and spinneret required to be heated to maintain the polymer in a liquid state. The fibers produced in melt spinning are typically found to have larger diameters than those from the polymer solutions due to the higher viscosity of a polymer melt than its solution. The apparatus used by Brown et al. [9] is depicted in .

[TODO: draw an apparatus used for melt electrospinning].

Despite the added complexity and thicker diameters, melt electrospinning gets around the need to handle volatile solvents, making the process safer to be performed on larger scales, On the other hand, this technique gets rid of any solvent contamination.

The first report of a melt electrospun drug delivery system came from Nagy et al. [10], who prepared fibers by melt electrospinning of Eudragit EPO with carvedilol. The drug and polymer were melted and mixed to form a homogeneous solid mixture prior to spinning. The melt-spun fibers reached diameters of 5–30 μm, compared to 300–1000 nm diameters produced from solution-spun fibers.

This work has been built on to blend plasticisers with the polymer Eudragit EPO and carvedilol active ingredient. [11] The plasticisers Triacetin, Tween 80 and Polyethylene Glycol were investigated by Attila et al. in order to reduce the melting point of the polymer-drug mixture. The temperature drop is desirable to minimize the occurring drug degradation.

Lian and Meng [12] performed a comparison of poly(ε-caprolactone) (PCL) fibers fabricated by the melt and solution electrospinning techniques. Lian and Meng [12] reported that melt spinning is preferable when the polymer presents a low solubility, on the other hand the melt fibers

were produced in a slower release rate. Lian and Men findings feature the solution-spun fibers to have a porous structure. Gernot et al. [13] demonstrated that submicron-size fibers are possible through melt electrospinning. In their effort, they achieved a precise deposition of PCL fibers with diameters of $817 \pm 165nm$.

In literature, melt electrospinning has less evidence than the solution approach. However, melt electrospinning arises to be as flexible as its solution counterpart in handling multiple polymers, as reported in McCann's work [14]. Currently, the melt electrospinning setup is harder to establish but the lack of research on this technique explains its unexplored potential.

1.3. Stretching forces

1.3.1. Electric Field

1.3.2. Centrifugal force

The spinning processes require the implementation of a force to break the polymer source into a polymer jet. Centrifugal spinning intends to produce fibers by the use of a rotating polymer source. The centrifugal force generated from typical rotatory speeds above 2000 rpm, results in fiber formation. [15, 16].

The centrifugal force technique is applied to polymer solutions and melts. This approach is used in applications were the precise deposition of the fibers is not relevant and production rate is to be maximized [17]. Efforts in centrifugal spinning are focused on drug delivery applications. Zander [18] fabricated polycaprolactone (PCL) fibers using the solution and melt variants of the centrifugal approach. Zander's fibers were produced with rotatory speed between three and 18 thousand revolutions per minute with $10\mu m$ in diameter.

On the other hand, PCL and PVP fibers were generated by Amalorpava et al. [19]. Amalorpava achieved sub micron/size fiber diameters for drug release purposes and bacteria growth inhibition properties. Literature [20] has shown that centrifugal approach has a simple setup that promises a large scale fabrication of fibers.

In some cases the centrifugal force implementations and pressurized gyration can be combined with an electric field. The implementation of two stretching forces (centrifugal and electrical forces), can help solvent evaporation [21]. Centrifugal electrospinning implements the same setup as the standard centrifugal spinning with the addition of a high voltage power supply between the rotating dispensing nozzle and the collector. The combined method has evidence to yield parallel fibers [22–25] at a higher rate [22, 23] than the standard electrospinning approach.

1.3.3. Blowing forces

Nano fibers can be produced with the implementation of pressurized gas with a polymer solution. The setup used for blow spinning is similar to the one used in standard electrospinning, where the polymer precursor is dispensed at a controlled rate. Unlike traditional electrospinning, in the solution blow spinning setup the needle nozzle applies pressurized gas to the polymer solution through an outer spinneret [26].

[TODO: draw an apparatus used for solution blow spinning or melt blowing] [26].

A few studies have explored solution blowing in drug delivery, with the first such work being from Oliveira et al. in 2013. [27] These authors prepared poly(lactic acid) (PLA) fibres loaded with the hormone progesterone, which can be used to regulate the reproductivecycle in livestock. Fibres were produced from solutions with 6% w/vPLA and between 0 and 8% w/v progesterone. The PLAis semi-crystalline both before and after processing, while the drug isamorphous post-spinning. The fibres behave very similarly in termsof their release behaviour, regardless of the amount of drug loaded.

A study comparing electrospun and solution-blown fibres of poly(3-hydroxybutyrate-co-3-hydroxyvalerate) loaded with sodium diclofenachas also been reported. [26] The drug-loaded fibres were slightly larger in diameter when generated by electrospinning, and the size uniformity was higher through solution blowing. In general there was a greateramount of burst release seen with the electrospun fibres, but otherwisethere were no clear trends in the drug release data.

Solution-blown fibres have additionally been

created loaded with oil extracted from the medicinal plant Copaifera sp., which is often explored for antimicrobial purposes. [28] These materials were constructed from a blend of the polymers PLA and PVP, and were around 1 μm in diameter. An increased PVP content was found to result in increased antibacterial activity after 24 h.

The melt blowing process has also received some attention in thepharmaceutical setting, and the fibres produced compared with thosefrom both solution and melt electrospinning. [29] Marosi's team generatedformulations from a vinylpyrrolidone–vinyl acetate copolymer, employingpoly(ethylene glycol) (PEG) as a plasticiser and carvedilol as a modeldrug. All three methods led to fibres, with the solution electrospun fibres narrowest (at 2 μm in diameter), followed by the melt-blown (10μm) and melt-spun (50 μm) products. Carvedilol was rendered into the amorphous physical form by all three processing techniques, and all theformulations were able to accelerate the drug dissolution process. Themelt-blown and melt electrospun systems led to the fastest release, withalmost identical release profiles, while the solution-electrospun fibresfreed their drug cargo somewhat more slowly.

A variant of the solution-blowing technique has been applied tothe processing of living cells (in this setting it has been referred to asbiothreading). [30] Using a pressurised coaxial needle with the exteriorfluid comprising a viscous polydimethylsiloxane solution and an aqueouscell suspension in the core, cells can be processed into scaffolds with nonoticeable loss in viability.

Electrospinning and melt/solution blowing can be combined in a processknown as electroblowing. This employs both electricity and a gas flow toaid fibre elongation and solidification. The experimental apparatus usesa similar spinneret to that in [Figure apparatus used for solution blow spinning or melt blowing], and in addition to the gas flowa potential difference is applied between the spinneret and the collector.This technique has been shown to have significant potential in medicalapplications: in 2014, Jiang et al. applied electroblowing in vitro and invivo to deliver a homogeneous and continuous layer of a medical glue tostop bleeding during liver resection. [31]

More recently, Balogh et al. prepared fibres of 2-hydroxypropyl-β-cyclodextrin loaded with sodium diclofenac. [32] They found that whenelectrospinning this system, very frequent clogging of the spinneretoccurred. Electroblowing overcame this issue and additionally allowedfaster flow rates to be used, increasing the amount of material thatcould be produced. However, the uniformity of the fibre products wascompromised, with more 'beads-on-string' type morphology seen withthe blown products. In both cases, the fibres comprised amorphous soliddispersions with no crystalline drug evident. The electroblown fibresdissolved a little more slowly than those from electrospinning, but stillmuch more rapidly than a physical mixture of drug and cyclodextrin.

A subsequent study using Eudragit E and itraconazole (anantifungal active pharmaceutical ingredient) also found that a fasterflow rate could be used in blowing, but that the fibre products from thelatter had less regular morphologies. [33] Again, the drug was amorphouslydispersed in the fibres, and the dissolution profiles of the electrospun andelectroblown systems were very similar.

1.3.4. Microfluidic forces

Microfluidic spinning is based on the use of micro (sub-millimetre)channels. A large number of these are located in a single microfluidicchip, and the rate and time of liquid expulsion from each channel are precisely controlled by computer. Microfluidic spinning can be coupled withelectrospinning, as described in detail in a recent review by Cheng et al. [51]While the productivity of microfluidic methods is a major challenge inscale-up, the technique offers the ability to generate fibres with a highlevel of complexity not easily achievable by electrospinning. For example,using a digitally programmed microfluidic flow, Kang et al. created functional microfibres with continuous spatiotemporal coding along thelength of the fibre. [52] The fibres contained varied chemical compositionsand topography, and localised bioactive agents.

Microfluidic spinning therefore has the poten-

tial to enable veryprecisely tuneable loading of different drugs into a single fibre, allowingfor programmable release in different parts of the body at differenttimes. The technique is beginning to be explored for drug deliveryapplications. However, the materials used in microfluidics are usuallyhydrogels (crosslinked polymer networks solvated with water). Theseoften have fast degradation rates and as a result can be unsuitable forthe extended release of drugs, particularly small molecules. To helpmitigate this problem, Chae et al. developed a microfluidic spinningmethod using an isopropyl alcohol sheath flow with an aqueousalginate core flow. [53] This innovation resulted in nanofibres made ofhighly ordered alginate molecules. Ahn et al. loaded ampicillin intoalginate fibres prepared in this manner, [54 and found that the orderedstructure delayed fibre degradation, allowing extended-release profileof ampicillin over 7 days.

1.3.5. Mechanical force

1.4. Dispensing nozzle: Coaxial / Monoaxial: Single nozzle / Multinozzle

1.5. Nozzle-to-substrate distance

1.5.1. Near Field Spinning

Figure 2 describes a typical near-field electrospinning set-up [5]. Two sub-techniques can be derived from electrospinning depending on the distance between the dispensing electrode and the collector. The process in which the electrospun jet can be controlled near the tip is called NFES or near-field electrospinning [27]. Moreover, if the distance between the collector and the dispensing needle is greater, the configuration is known as FFES or far-field electrospinning [28].

1.5.2. Far Field Spinning

In a far field electrospinning the process continues ... Decreasing the jet diameter, the surface charge density increases and the resulting high repulsive forces split the jet into several smaller jets. The jet is seriously elongated by a bending and whipping processes caused by electrostatic repulsion initiated at small bends in the fiber, until it is finally deposited on the collector. Two types of collector may be used, either stationary or rotary collector.

2. "Electro - DC - monoaxial - solution - NF - spinning"

Near-field electrospinning is considered to be an outstanding technique to fabricate polymer fibers with spatial control and it has suffered several modifications to improve the precision and accuracy of the fiber deposition. This paper intents to collect the NFES variants of electrospunable polymer solutions with spatial control in recent research.

Nanofibers are fibers with diameters in the nanometer range. The development of nanofibers has greatly enhanced the scope for meeting up the modern world challenges.

Currently there are two types of electrospinning systems available for producing nanofiber: needle based electrospinning and needleless electrospinning. This paper summarizes the basic mechanism of various types of needle based and needleless spinning systems described in various literatures by many researchers.

2.1. Low-Voltage NFES (LV NFES) [29]

Some differences have been discovered between LV-NFES and conventional NFES. Low voltage near field electrospinning produces thinner fibers with lower voltages. Moreover, when implementing a moving stage, the fibers are affected by the mechanical stretching. Bisht et al. [29] reported that thinner diameters are yield with the increase of the x-y stage velocity, and larger diameters by decreasing the stage velocity.

2.2. Scanning Tip Electrospinning [30]

Lorem ipsum dolor sit amet, consectetur adipiscing elit, sed do eiusmod tempor incididunt ut labore et dolore magna aliqua.

2.3. 3D Electrospinning [31]
Electrohydro-dynamic 3D Print-patterning or Electrohydro-dynamic Jetting [32]

Lorem ipsum dolor sit amet, consectetur adipiscing elit, sed do eiusmod tempor incididunt ut labore et dolore magna aliqua.

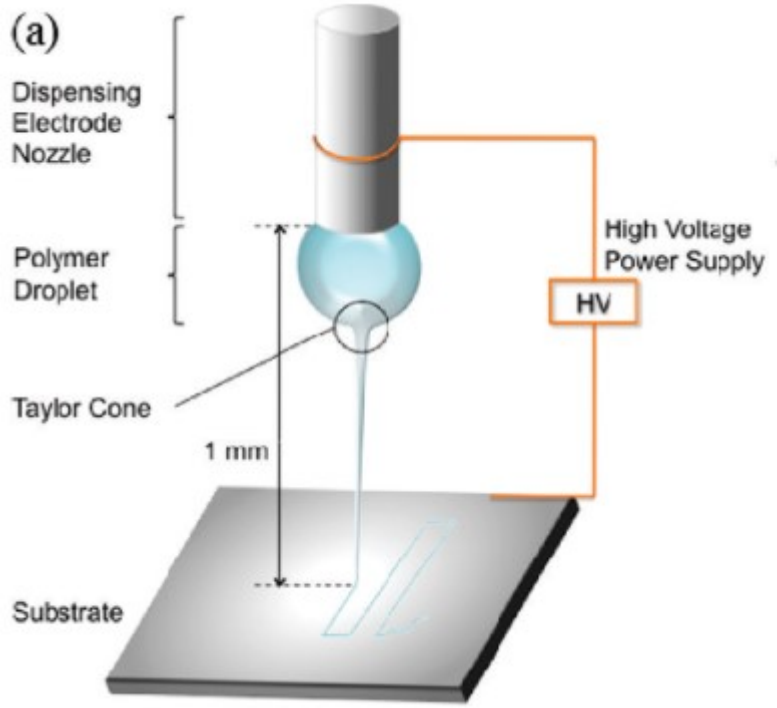

Figure 2: Typical near-field electrospinning set-up [29] .

2.4. Multinozzle NFES [33–35]

Lorem ipsum dolor sit amet, consectetur adipiscing elit, sed do eiusmod tempor incididunt ut labore et dolore magna aliqua.

2.5. Electrohydro-dynamic Writing or Mechano-electrospinning (MES) [36]
Electrohydro-dynamic Direct-Write (EDW) [37]
Mechano-Electrospinning [38]

Lorem ipsum dolor sit amet, consectetur adipiscing elit, sed do eiusmod tempor incididunt ut labore et dolore magna aliqua.

2.6. Suspension NFES [39]

Lorem ipsum dolor sit amet, consectetur adipiscing elit, sed do eiusmod tempor incididunt ut labore et dolore magna aliqua.

2.7. Helix Electrohydro-dynamic Printing (HE-printing) [40]
Electrohydro-dynamic (EHD) jet printing [41]

Lorem ipsum dolor sit amet, consectetur adipiscing elit, sed do eiusmod tempor incididunt ut labore et dolore magna aliqua.

2.8. Airflow-assisted Electrohydro-dynamic Direct-writing (EDW) [42]

Lorem ipsum dolor sit amet, consectetur adipiscing elit, sed do eiusmod tempor incididunt ut labore et dolore magna aliqua.

2.9. Tethered Pyro-Electrohydro-dynamic Spinning (TPES) [43]

Lorem ipsum dolor sit amet, consectetur adipiscing elit, sed do eiusmod tempor incididunt ut labore et dolore magna aliqua.

3. Polymer Solution

In electrospinning, it is typically agreed that the diameter of the fibers increased with higher concentration due to greater viscosity which withstands stretching. In near field electrospinning, similar observations have been reported where concentration increases, fiber diameter increased [30, 44]. However, in separate studies by Pan et al. [45, 46] using poly(γ-benzyl α, l-glutamate) and polyvinylidene fluoride (PVDF) reported reduction in fiber diameter with increasing concentration.

Table 1: Approximation process to estimate the critical polymer concentration. Several polymer concentrations are tried and the resulting jets are observed until a continuous stream is achieved.

Observation	Concentration Adjustement
Dripping, no stream	Increase
Splitting small droplets	Increase slightly
Steady stream	No concentration adjustment
Splitting large globs	Decrease slightly
Nozzle clogging	Decrease

3.1. Polymers

The polymer selection is in function on the intended application. For example, a fast dissolving hydrophilic polymer such as poly(ethylene oxide) (PEO) is used for fast drug delivery systems. Otherwise, slow dissolving polymers such as poly(ε-caprolactone) (PCL) or poly(lactic-co-glycolic acid) (PLGA) are implemented. [47]

The polymer molecular weight along with the polymer concentration and solvent selection have a direct effect on the solution viscosity, conductivity and surface tension, hence the solution behavior in the electrospinning process. The spunable viscosity range varies with the polymer and solvent.

Solutions with low viscosity are prone to insufficient polymer chain entanglements to produce fibers. [47] On the other hand, if the solution is too viscous, then the surface tension cannot easily be overcome by the electric field. In both cases, the result can be droplets or particles forming rather than fibers; see Table 1.

3.2. Solvents

The solvent used must be capable of dissolving the polymer of interest at an appropriate concentration to form fibers, and must posses a suitable volatility. A low-volatility solvent like water may fail to evaporate completely over the distance between the spinneret and the collector. When the fibers form, they will hence contain residual water owing to this incomplete evaporation. The residue solvent will subsequently evaporate from the fibers upon storage, resulting in ribbon-like (flattened) fibers, wrinkles on the fiber surface or fused fibers. On the other hand, a high-volatility solvent may evaporate very quickly, leading to larger fiber diameters (less time for elongation before solidification) and clogging of the spinneret (due to drying of the liquid at the spinneret before jetting, or drying of the Taylor cone during jetting). Solvents commonly used for electrospinning include ethanol, chloroform, dichloromethane and hexafluoroisopropanol.

Mixtures of miscible solvents can be used to ensure that sufficient polymer can be dissolved to give a solution of appropriate viscosity and volatility with suitable dielectric constant range to allow fiber formation. However, care must be taken because using a mixture of solvents with very different volatilities can result in porous fiber structures, as reported by Katsogiannis et al. for organic solvent mixtures with dimethyl sulfoxide (DMSO). [48] DMSO evaporates much more slowly than the organic solvents used, which results in its incorporation into the fibers. The DMSO will eventually evaporate, yielding porous fibers.

It is also important to take into account the surface tension of the solution. Solvents with very high surface tensions (e.g. water) can result in instability arising during the spinning process, and a broad range of fiber diameters in the products. If necessary, a surfactant can be added to reduce the surface tension, but this will be incorporated into the fibers produced.

4. Effect of the NFES Parameters

To spin nano fibers at close distances, the initial diameter of the jet is required to be as small as possible since stretching of the thread is limited.

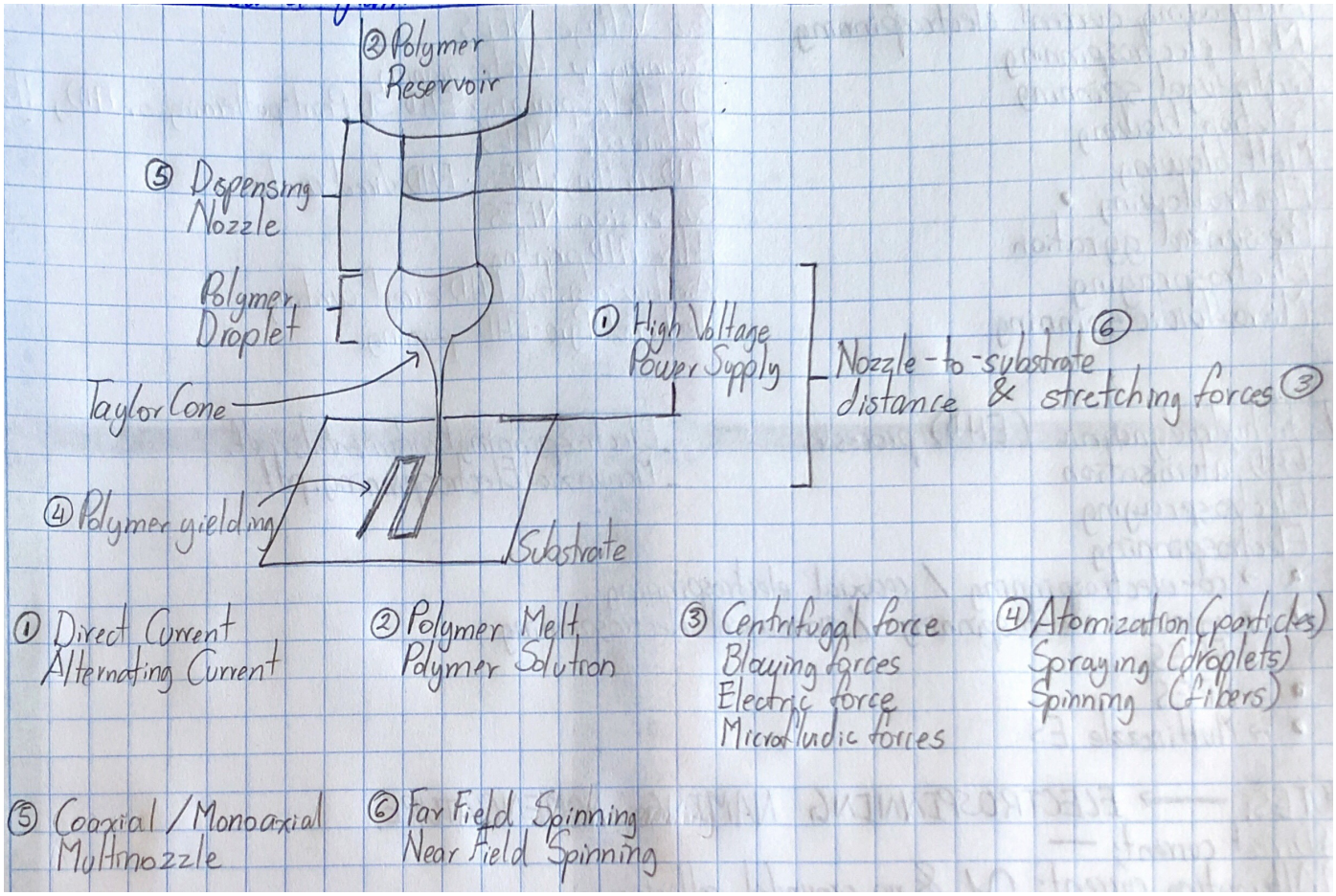

Figure 3: Near-Field ES Process Parameters

Kameoka et al. [49] demonstrated that a small initial spinning radius can be achieved using an atomic force microscope tip with a small polymer solution drop at the tip.

Near-field electrospinning, has exhibited to be capable fabricate nano fibers over and nano fiber patterns [50]. Nevertheless, having a small polymer solution drop at the nozzle tip limits the length of the fibers that can be fabricated in a continuous manner. Using a spinneret with a reservoir (e.g. syringe) of solution generally produces fibers with diameter of a few micrometers [32, 51], since it creates a limit to which the nozzle inner diameter can be reduced to allow the solution to flow through.

Coppola et al. [43] have showed a NFES variant that allows polymer nano fibers to be deposited directly from a polymer drop, averting the issue of nozzle clogging. The fibers are also prone soaking after deposition thus giving the fibers a semi-circular cross-section as depicted in Xue et al.'s [51] work.

4.1. Nozzle spinneret

The thinnest nozzles in literature so far are about 100 μm in diameter, for instance Chang et al. [30] used a 100 μm inner diameter needle tip to electrospin poly(ethylene oxide) (PEO) and Camillo et al. [52] used a micro-diameter tip Tungsten spinneret in a 26G needle to electrospin co-polymer, poly[2-methoxy-5-(2-ethylhexyloxy)-1,4-phenylenevinylene] (MEH-PPV) with poly(ethylene oxide) (PEO). The nozzle most commonly comprises a simple narrow-bore, blunt-end metal needle. The diameter of the needle can vary, but most commonly researches work with internal diameters below 1 mm . This translates to needles of gauge 18–22.

In general, this simple spinneret design can be used to achieve successful spinning. A blunt-end rather than a tapered-end for the needle exit is important as the size distribution of the products increase with an increase in needle tip angle. However, it should be noted that there will be some interactions between the solvent and polymer molecules in the solution and the metal surface of the spinneret. There will exist some attractive forces between the polar groups in the polymer and the electropositive metal surface, which can act counter to the drawing force of the electric field and can pull the polymer solution back into the spinneret. It has been found that coating the spinneret exterior in a non-conductive and non-stick polymer such as Teflon can reduce these interactions. [53] As a result, the electrical energy can be more efficiently used to elongate and narrow the polymer jet, and narrower fibers can be produced. In addition, strong attractive forces between the polymer jet and the metal spinneret can result in fibers becoming attracted to the needle, leading to lower yields and potentially to blocking of the exit orifice. This effect too can be ameliorated using an epoxy coating. [54]

4.2. Applied Voltage

In recent literature, near field electrospinning has been studied to reduce the fiber diameter and to improve the fiber deposition accuracy. Camillo et al. [52] demonstrated that the application of a modified fine tip nozzle enables the fabrication of 100 nm diameter fiber at a nozzle-to-substrate distance of 500 μm and an applied voltage of 1.5 kV . On the other hand, Bisht et al. [29] and Chang et al. [30] came to the conclusion higher voltages yield thicker micro-fibers with a loss in jet stability.

This discrepancy in literature between the applied voltage and resulting fiber diameter is due to the relationship with other variables such as nozzle-to-substrate distance and solution deposition rate. For instance, if a high voltage is applied at a low deposition rate then electrospraying is achieved, meaning the formation of several non-continuous fibers. The applied voltage shall be sufficient to break the surface tension and initiate the jet, but low enough to avoid multiple jets at the nozzle tip.

Bisht et al. [29] achieved the fabrication of thinner fibers with spatial control by reducing the applied voltage to 200-600 V at a nozzle-to-substrate distance of 0.5-1 mm. The low voltage setting does not create enough charge to break the polymer solution surface tension to initiate the electrospinning process.

Bisht et al. [29] and Chang et al. [30] initiated the electrospun fibers by mechanically pull the polymer solution at the nozzle tip using a microprobe tip. Chang and coworkers reduced the applied voltage from 1.5 kV to 600 V with a nozzle-to-substrate distance of 500 μm to yield a fiber diameter between 3 μm and 50 nm . With an applied voltage of 200 V and a nozzle-to-substrate distance of 1 mm , PEO nano fibers were deposited with a diameter about 20 nm.

In near-field electrospinning, the applied voltage has an impact on the produced fiber morphology. For instance, a voltage higher or lower to the optimum voltage will translate into an increase in fiber diameter. Song et al. [41] demonstrated that a decrease in voltage from 400 to 500 V can reduce the fiber diameter from 160 to about 60 $nm$with a nozzle-to-substrate distance of 20 μm. The optimum voltage is achieved when a balance is attained between the stretching of the jet and the speed at which it hits the substrate. The increase of voltage yields thinner fibers as it causes greater stretching, and a greater jet acceleration.

Another workaround to break the polymer solution surface tension is to initialize the NFES process with a higher voltage and then lower the voltage once the jet is created. Huang et al. [36] implemented the previous and yield ordered fibers with a distance between adjacent fibers of 50 μm. In most cases, a positive voltage is applied to the spinneret.

4.3. Nozzle-to-substrate distance

In NFES, the fiber morphology can be altered by the control of the height between the nozzle and the substrate (collector). With the decrease of the nozzle-to-substrate distance, the electric

field strength increases; however it can cause incomplete solvent volatilisation and possible short circuits between the collector and the nozzle tip.

An optimal nozzle-to-substrate distance shall be defined to ensure the fabrication of dry continuous fibers. If the solvent is not well evaporated, the produced fibers are prone to defects; on the other hand if solidification happens too fast, the solids can block the spinneret which can prevent a continuous fiber yield. Furthermore, the polymer jet will discharge itself as soon as possible, therefore long distances can result in low yields.

Typically, metal nozzle tips are used, with small inner diameters. From literature, needles with small diameters produce thinner fibers. A thin nozzle tip can help the reduction of the fiber diameter, but also it is more likely to become blocked.

4.4. Electric field

Recent literature suggests that the fiber morphology depends on the electric field profile created by the applied voltage during NFES. Since the electric field is an induced force that attracts the solution jet towards the desired location within the collector.

Bisht et al. [29] and Min et al. [55] have reported the ability to electrospin nano fibers with high accuracy. Min et al. [55] implemented a NFES setup with multiple "field-effect transistors" on a flexible polyacrylate collector with an x-y stage velocity of 13.3 cm/s to fabricate fibers with a diameter about 289 nm and a distance between adjacent fibers of 50 μm.

On the other hand, Bisht et al. [29] showed evidence of fabricated fibers with low-voltage NFES with high accuracy and precision. Bisht et al.'s suspended fibers were deposited over carbon posts with a distance between adjacent fibers of 100 μm with diameter of 30 μm [29].

The employment of guided electrodes in NFES, adapts the fabrication process to yield a more accurate fiber deposition. For instance, Kim et al. [31] manufactured ink patterns on a paper with silver nano particles. The printed patterns aid the fibers to land on the desired location. Kim et al. [31] electrospun the fibers with a distance between adjacent fibers of 150 μm.

Xu et al. [56] created a straight jet from the nozzle tip to the substrate using a guiding electrode underneath the collector. The purpose of the guiding electrode is to adjust the path of the NFES jet. With the guiding electrode implementation, the fiber's spread was reduced from 74 μm to 7 μm.

4.5. Substrate

Due to the close distance between the grounded substrate and the charged spinneret in NFES, the set up is prone to electrical shorts. In NFES, when a short circuit takes place, the electrospinning process is interrupted resulting in the fabrication of discontinuous fibers. Two workarounds to avoid electrical shorts is to lower the applied voltage and to install less conductive substrates [57, 58].

Liu et al. [57] discovered that the fiber alignment is improved by using a glass-cooper foil substrate, however the well aligned fibers are spoiled after prolonged depositions due to residual charges. Additionally, the effect of residual charges is amplified with the used collector substrate contains a conductive layer and a non-conductive layer [57].

On the other hand, Choi et al. [58] implemented a hydrophobic substrate to deposit the fibers with plasma treatment to increase the conductivity of selected areas. NFES was carried put with precise deposition as the fibers were placed as per the desired design within the hydrophilic substrate.

Table 2: Electrospun Polymer Solutions - Solution and Process Parameters

Polymer(s)	Solvent(s)	NFES Variant	Process Parameters and Fiber Characterization	Ref.
Poly(ethylene oxide) (PEO; MW = 4,000,000 g/mol)	Deionized water	Low-Voltage NFES (LV NFES)	**Solution Concentration:** 1, 2, and 3 $wt\%$ PEO **Nozzle:** 27 gauge type 304; stainless steel needle **Solution deposition rate:** lower than $1\mu L/h$ **Nozzle-to-substrate distance:** $1mm$ **Substrate composition:** Pyrolyzed SU-8 carbon and Si **Applied voltage:** polymer jet initiated at 400-600 V and dispensed at 200-400 V **x-y stage velocity:** 10-40mm/s **Fiber Diameter:** 50-425nm **Distance between adjacent fibers:** *Not determined*	[29]
Poly[2-methoxy-5-(2-ethylhexyloxy)-1,4-phenylenevinylene] (MEH-PPV; MW = 380,000 g/mol) with Poly(ethylene oxide) (PEO; MW = 300,000 g/mol)	acetonitrile toluene mixture (65/35); acetic acid toluene (17/83); pure toluene	Typical NFES process	**Solution Concentration:** $10mg$ of MEH-PPV in $2mL$ of toluene; $500\mu L$ of MEH-PPV solution with $250mg$ of PEO in $3.5mL$ of acetonitrile / toluene (65 / 35); $500\mu L$ of MEH-PPV solution with $250mg$ of PEO in $3mL$ of acetic acid / toluene (17 / 83). The resulting MEH-PPV/PEO concentration is 0.08 $wt\%$ **Nozzle:** mm-diameter tip Tungsten spinneret in a 26 gauge needle **Solution deposition rate:** $50\mu L/h$ **Nozzle-to-substrate distance:** $500\mu m$ **Substrate composition:** SiO2/Si (oxide thickness = 800 nm) **Applied voltage:** around $1.3kV$ **x-y stage velocity:** $50cm/s$ **Fiber Diameter:** $100nm$ **Distance between adjacent fibers:** around $100\mu m$	[59]

Continued on next page

Table 2 continued

Poly(ethylene oxide) (PEO; MV = 300,000 g/mol)	Water	Scanning Tip Electrospinning and NFES	**Solution Concentration:** $7wt\%$ PEO **Nozzle:** Needle outer diameter of $200\mu m$ and inner diameter of $100\mu m$ **Solution deposition rate:** $0.1\mu L/h$ **Nozzle-to-substrate distance:** $500\mu m$ **Substrate composition:** *Not determined* **Applied voltage:** polymer jet initiated at 1.5 kV and dispensed at $600V$ **x-y stage velocity:** $120mm/s$ **Fiber Diameter:** $709\pm131nm$; 49-74nm when applied voltage is $800V$ **Distance between adjacent fibers:** *Not determined* **Notes:** $108m$ yield in $15min$ with a fiber diameter of $709\pm131nm$	[30]
Poly(vinylidine fluorid) (PVDF; MW = 440,000 g/mol)	N,N Dimethylformamide (DMF)	Helix Electrohydrodynamic Printing (HE-printing)	**Solution Concentration:** $1.8g$ PVDF in $4.1g$ of DMF and $4.1g$ of acetone. The resulting concentration is 18% PVDF. **Nozzle:** Needle outer diameter of $510\mu m$ and inner diameter of $260\mu m$ **Solution deposition rate:** $400nL/min$ **Nozazle-to-substrate distance:** 10-50mm **Substrate composition:** Poly(dimethylsiloxane) (PDMS) on Ecoflex **Applied voltage:** 1.5–3kV **x-y stage velocity:** 0-400mm/min **Fiber Diameter:** about 1.5-3μm **Distance between adjacent fibers:** *Not determined*	[40]

Continued on next page

Table 2 continued

Polyhedral Oligomeric Silsesquioxane-Poly(Carbonate-Urea)Urethane (POSS-PCU) and Polyhedral Oligomeric Silsesquioxane Poly(Caprolactone-Poly(Carbonate-Urea)Urethane) (POSS-PCL-PCU) (Dry Polycarbonate MW = 2000 g/mol)	Dimethyl acetamide (DMAC) and 1-Butanol	Electrohydrodynamic 3D Printpatterning or Electrohydrodynamic Jetting	**Solution Concentration:** POSS-PCU and POSS-PCL-PCU used in 20%w/w concentration in DMAC **Nozzle:** needle of 750 μm in diameter **Solution deposition rate:** less than 1$\mu L/min$ **Nozzle-to-substrate distance:** about between 500μm to 2mm **Substrate composition:** *Not determined* **Applied voltage:** 8.0-10.0kV **x-y stage velocity:** 10mm/s **Fiber Diameter:** 5-50μm **Distance between adjacent fibers:** 250μm	[32]
Poly(ethylene oxide) (PEO; MW = 300,000 g/mol)	Distilled water	Electrohydrodynamic Writing or Mechanoelectrospinning (MES)	**Solution Concentration:** 6wt% PEO **Nozzle:** *Not determined* **Solution deposition rate:** 1200nL/min **Nozzle-to-substrate distance:** 7.5mm **Substrate composition:** *Not determined* **Applied voltage:** polymer jet initiated at 2 kV and dispensed at 0.8-1kV **x-y stage velocity:** around 400mm/s **Fiber Diameter:** 200-350nm **Distance between adjacent fibers:** 5μm	[36]

Continued on next page

Table 2 continued

Poly(ethylene oxide) (PEO; MW = 300,000 g/mol)	Deionized water and ethanol with a volume ratio of 3:1	Airflow-assisted Electrohydrodynamic Direct-writing (EDW)	**Solution Concentration:** $8wt\%$ PEO **Nozzle:** Outer airflow passage diameter: $1mm$ Airflow gas pump pressure: $25kPa$ Inner liquid passage diameter: $0.21mm$ **Solution deposition rate:** $30\mu L/h$ **Nozzle-to-substrate distance:** $2mm$ **Substrate composition:** Silicon **Applied voltage:** about $2kV$ **x-y stage velocity:** 1-$20mm/s$ **Fiber Diameter:** $3.73 \pm 1.37\mu m$ **Distance between adjacent fibers:** $5.13 \pm 6.67\mu m$	[42]
Poly(Vinylidene Fluoride) (PVDF; MW = 534,000 g/mol)	Acetone and Dimethyl Sulfoxide (DMSO)	3D Electrospinning	**Solution Concentration:** $17wt\%$ PVDF; $1.7g$ of PVDF, $5g$ of acetone, $0.5g$ of Capstone FS-66, $5g$ of DMSO **Nozzle:** Needle inner diameter of $100\mu m$ **Solution deposition rate:** $14\ nL/min$ **Nozzle-to-substrate distance:** $750\mu m$ **Substrate composition:** A4 size commercial printing paper (Double A) **Applied voltage:** $1.9kV$ **x-y stage velocity:** $10mm/s$ **Fiber Diameter:** *Not determined* **Distance between adjacent fibers:** *Not determined*	[31]
Poly(9-Vinyl Carbazole) (PVK; MW = 1,100,000 g/mol)	Styrene	Typical NFES process	**Solution Concentration:** $3.96wt\%$ PVK in styrene **Nozzle:** Needle inner diameter of $100\mu m$ **Solution deposition rate:** $500nL/min$ **Nozzle-to-substrate distance:** around $2.5mm$ **Substrate composition:** Si/SiO2 **Applied voltage:** 3-$4kV$ x-y stage velocity: $13.3cm/s$ **Fiber Diameter:** $289.26 \pm 35.37nm$ **Distance between adjacent fibers:** $50\mu m$ **Notes:** $15m$ yield in $2min$	[55]

Continued on next page

Table 2 continued

Polystyrene (PS; MW *Not determined*)	1,2,4-Trichloro benzene	Electrohydrodynamic (EHD) jet printing	**Solution Concentration:** 1 to 5wt% PS **Nozzle:** Glass nozzle inner diameter of 2μm and outer diameter of 2.66μm **Solution deposition rate:** *Not determined* **Nozzle-to-substrate distance**: 20, 30, 40μm **Substrate composition:** Si **Applied voltage:** 500 to 400V in 25V increments **x-y stage velocity:** 0.01-10mm/s **Fiber Diameter:** about 60-170μm **Distance between adjacent fibers:** *Not determined*	[41]
Poly(ethylene oxide) (PEO; MW = 300,000 g/mol)	*Not determined*	Typical NFES process	**Solution Concentration:** 3wt% PEO **Nozzle:** *Not determined* **Solution deposition rate:** *Not determined* **Nozzle-to-substrate distance:** 500μm **Substrate composition:** Si **Applied voltage:** 1000V **x-y stage velocity:** 20cm/s **Fiber Diameter:** 300nm **Distance between adjacent fibers:** 25μm	[50]
Poly(ethylene oxide) (PEO; MW = 2,000,000 g/mol)	Distilled water	Multinozzle NFES	**Solution Concentration:** 5wt% **Nozzle:** four-nozzle and six-nozzle array with needle spacing changes from 1.5mm to 3.5mm **Solution deposition rate:** 1-3$\mu L/min$ **Nozzle-to-substrate distance:** 2mm **Substrate composition:** *Not determined* **Applied voltage:** 1.7-2.7kV **x-y stage velocity:** *Not determined* **Fiber Diameter:** 5.47μm **Distance between adjacent fibers:** 3-5 mm	[33]

Continued on next page

Table 2 continued

Poly(ethylene oxide) (PEO; MW = 2,000,000 g/mol)	Distilled water	Multinozzle NFES	**Solution Concentration:**5$wt\%$ **Nozzle:** Dual-28G-needle array with needle inner diameter of 0.18mm and outer diameter of 0.36mm; with needle spacing changes from 2.0mm to 3.0mm **Solution deposition rate:** 0.2$\mu L/min$ **Nozzle-to-substrate distance:** 3.0-4.0mm **Substrate composition:** *Not determined* **Applied voltage:** 2.0-3.0kV **x-y stage velocity:** 20mm/s **Fiber Diameter:** *Not determined* **Distance between adjacent fibers:** 218-326μm	[34]
Poly(ethylene oxide) (PEO; MW = 2,000,000 g/mol)	Distilled water	Multinozzle NFES	**Solution Concentration:**5 $wt\%$ **Nozzle:** Dual-28G-needle array with needle inner diameter of 180μm and outer diameter of 360μm; with needle spacing changes of 2.0mm **Solution deposition rate:** 0.2$\mu L/min$ **Nozzle-to-substrate distance:** 4.0mm **Substrate composition:** chromium-plated glass **Applied voltage:** 2.5kV **x-y stage velocity:** 20mm/s **Fiber Diameter:** *Not determined* **Distance between adjacent fibers:** 2.3002-2.7224mm	[35]
Poly(ethylene oxide) (PEO; MW = 4,000,000 g/mol)	*Not determined*	Typical NFES process	**Solution Concentration:** 2$wt\%$ **Nozzle:** G30 needle with inner diameter of 0.15mm **Solution deposition rate:** *Not determined* **Nozzle-to-substrate distance:** 1-3mm **Substrate composition:** Silicon **Applied voltage:** 1250V **x-y stage velocity:** *Not determined* **Fiber Diameter:** *Not determined* **Distance between adjacent fibers:** 20μm	[56]

Continued on next page

Table 2 continued

Gelatin (porcine skin; MW *Not determined*)	Acetic Acid and Ethyl Acetate	Typical NFES process	**Solution Concentration:** 11wt% gelatin, 30wt% water, 35.4wt% acetic acid, 23.6wt% ethyl acetate **Nozzle:** 19G needle tip with outer diameter of 1.08mm **Solution deposition rate:** *Not determined* **Nozzle-to-substrate distance:** 1.25mm **Substrate composition:** Poly(Dimethylsiloxane) (PDMS) films **Applied voltage:** 1000V **x-y stage velocity:** *Not determined* **Fiber Diameter:** around 2-3μm **Distance between adjacent fibers:** 40μm	[51]
Poly(ethylene oxide) (PEO; MW = 300,000 g/mol)	Water/Ethanol (v/v = 60/40)	Typical NFES process	**Solution Concentration:** PEO concentrations of 16% and 18% **Nozzle:** 40μm **Solution deposition rate:** *Not determined* **Nozzle-to-substrate distance:** 1mm **Substrate composition:** Planar silicon **Applied voltage:** 1.7kV **x-y stage velocity:** 0.36m/s **Fiber Diameter:** 5.15μm **Distance between adjacent fibers:** *Not determined*	[60]
Poly(ethylene oxide) (PEO; MW = 300,000 g/mol)	Water/Ethanol (v/v = 3/1)	Electrohydrodynamic Direct-Write (EDW)	**Solution Concentration:** 14wt% PEO **Nozzle:** Stainless needle with inner diameter of 210μm and outer diameter of 400μm **Solution deposition rate:** 50$\mu L/h$ **Nozzle-to-substrate distance:** 2mm **Substrate composition:** Poly(ethylene terephthalate) (PET) **Applied voltage:** 3kV **x-y stage velocity:** 700mm/s **Fiber Diameter:** 15-35μm **Distance between adjacent fibers:** 70μm	[37]

Continued on next page

Table 2 continued

Poly(ethylene oxide) (PEO; MW = 300,000 g/mol)	Deionized water	Mechano-Electrospinning	**Solution Concentration:** $3wt\%$ PEO **Nozzle:** Stainless steel nozzle with inner diameter of $160\mu m$ and outer diameter of $310\mu m$ **Solution deposition rate:** $50nL/min$ **Nozzle-to-substrate distance:** 2-5mm **Substrate composition:** Silicone **Applied voltage:**polymer jet initiated at $2kV$ and dispensed at $1kV$ **x-y stage velocity:** 200-400mm/s **Fiber Diameter:** from 344±32 to 214±27nm **Distance between adjacent fibers:** *Not determined*	[38]
Poly(co-Glycolic) acid (PLGA; MW *Not determined*)	Dimethyl Carbonate (DMC)	Tethered Pyro-Electrohydrodynamic Spinning (TPES)	**Solution Concentration:** *Not determined* **Nozzle:** nozzle-free **Solution deposition rate:** The drop reservoir is placed directly on a flat substrate **Nozzle-to-substrate distance:** Taylor's cone is focused and put in direct contact with the collector **Substrate composition:** Poly(tetrafluoroethylene) (PTFE) coated glass slide **Applied voltage:** pyro-electric field of between 2.7 $x10^7$ V/m and $5.5x10^7$ V/m **x-y stage velocity:** *Not determined* **Fiber Diameter:** 304.7nm **Distance between adjacent fibers:** *Not determined*	[43]

Continued on next page

Table 2 continued

Poly(ethylene oxide) (PEO; MW = 4,000,000 g/mol) with Tetrabutylammonium tetrafluoroborate (TBF; MW *Not determined*) and SU-8 2002	N,N Dimethylformamide (DMF)	Typical NFES process	**Solution Concentration:** SU-8/PEO/TBF blend with 0.75wt% PEO, 1wt% TBF; the blend is diluted with 30vol% DMF $\mu m \mu m$ **Solution deposition rate:** *Not determined* **Nozzle-to-substrate distance:** *Not determined* **Substrate composition:** Brass disk with a diameter of 38mm **Applied voltage:** 980V **x-y stage velocity:** *Not determined* **Fiber Diameter:** *Not determined* **Distance between adjacent fibers:** *Not determined*	[27]
Poly(ethylene oxide) (PEO; 200,000 g/mol)	Water:Ethanol (3:2)	Suspension NFES	**Solution Concentration:** 14wt% PEO **Nozzle:** stainless steel needle (25 G) with inner diameter of 0.25mm **Solution deposition rate:** 3nL/s **Nozzle-to-substrate distance:** between 0.5 and 10mm with 0.5mm increments **Substrate composition:** Planar silicon electrodes **Applied voltage:** 1.6kV **x-y stage velocity:** 50, 150, and 250mm/s **Fiber Diameter:** 300nm **Distance between adjacent fibers:** 0.1 and 0.5mm	[39]
Poly(ethylene oxide) (PEO; MW = 400,000 g/mol)	Deionized water	Typical NFES process	**Solution Concentration:** 10wt% PEO **Nozzle:** 32G metal needle **Solution deposition rate:** (Jet impact speed of 5mm/s) **Nozzle-to-substrate distance:** 0.5mm **Substrate composition:** p-type silicon wafer **Applied voltage:** 400V **x-y stage velocity:** 5mm/s **Fiber Diameter:** *Not determined* **Distance between adjacent fibers:** 50μm	[61]

5. Conclusion

Lorem ipsum dolor sit amet, consectetur adipiscing elit, sed do eiusmod tempor incididunt ut labore et dolore magna aliqua. Ut enim ad minim veniam, quis nostrud exercitation ullamco laboris nisi ut aliquip ex ea commodo consequat. Duis aute irure dolor in reprehenderit in voluptate velit esse cillum dolore eu fugiat nulla pariatur. Excepteur sint occaecat cupidatat non proident, sunt in culpa qui officia deserunt mollit anim id est laborum.

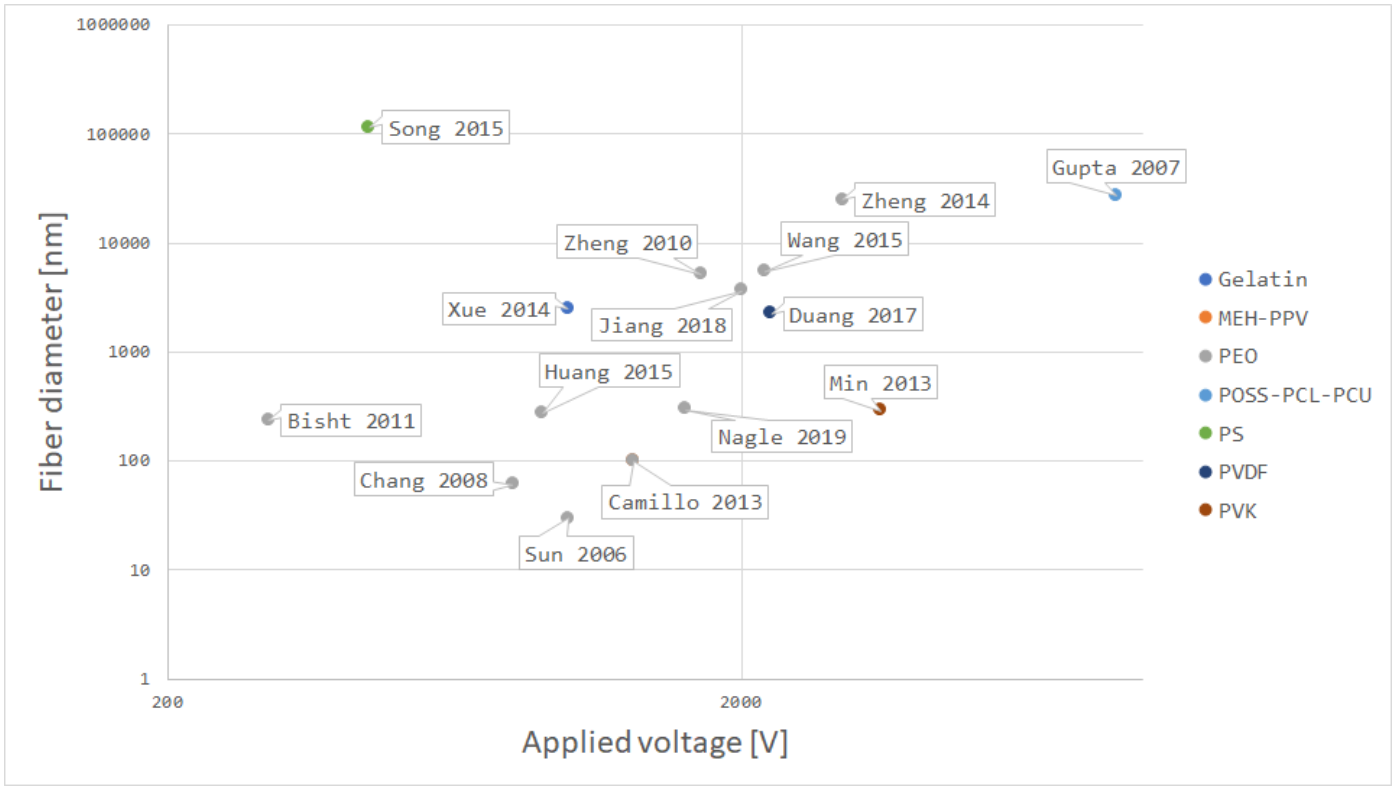

Figure 4: Applied volage vs. Fiber diameter

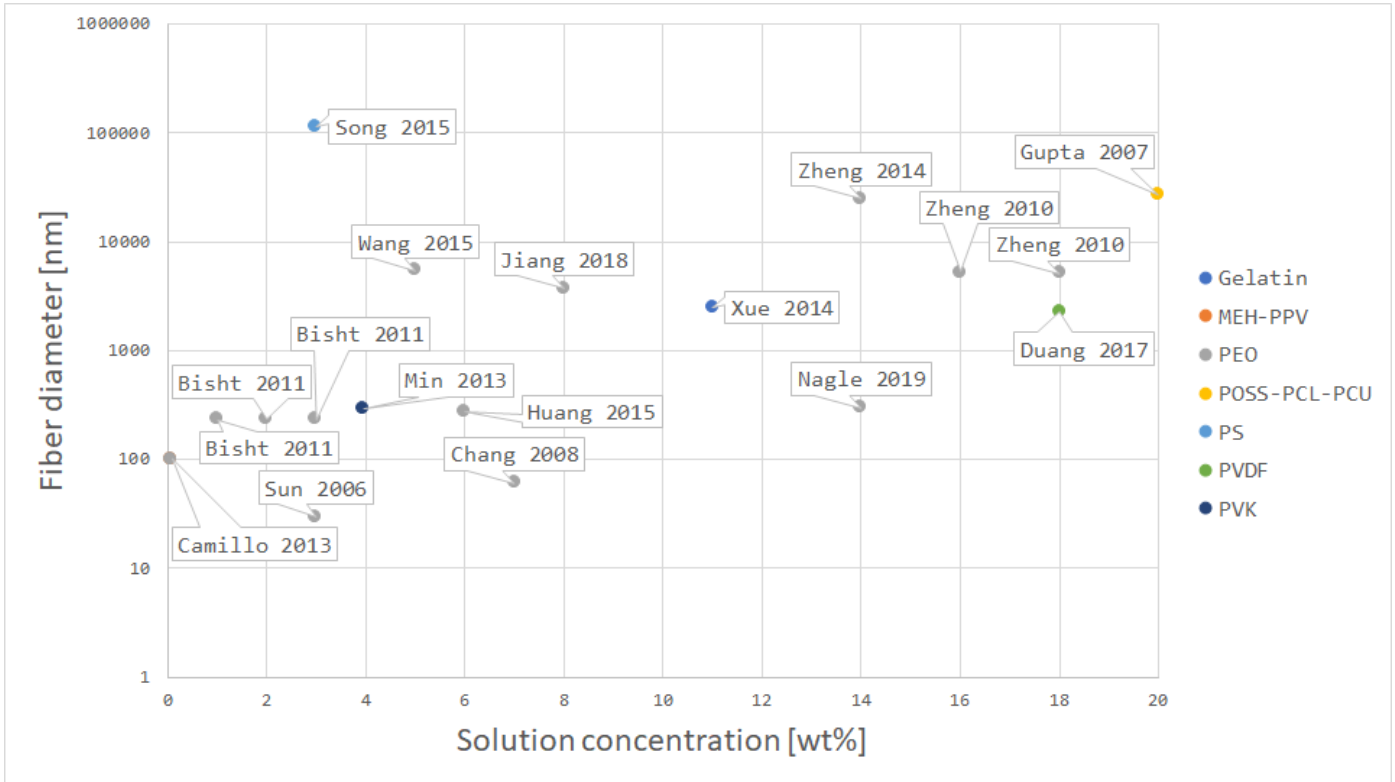

Figure 5: Solution concentration vs. Fiber diameter

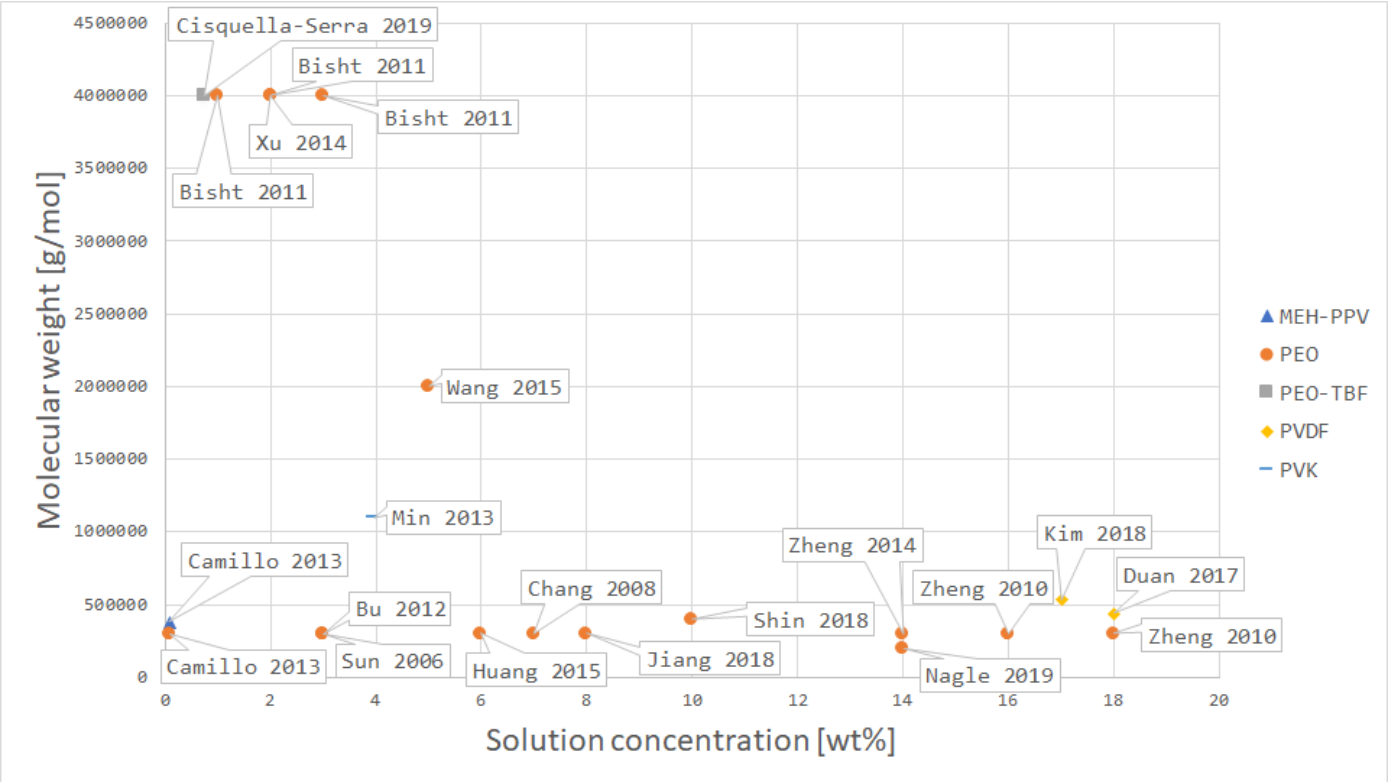

Figure 6: Solution concentration vs. Molecular weight

6. NFES Achievements & Challenges

Lorem ipsum dolor sit amet, consectetur adipiscing elit, sed do eiusmod tempor incididunt ut labore et dolore magna aliqua. Ut enim ad minim veniam, quis nostrud exercitation ullamco laboris nisi ut aliquip ex ea commodo consequat. Duis aute irure dolor in reprehenderit in voluptate velit esse cillum dolore eu fugiat nulla pariatur. Excepteur sint occaecat cupidatat non proident, sunt in culpa qui officia deserunt mollit anim id est laborum.

References

[1] F. Anton, Process and apparatus for preparing artificial threads (1930). doi:https://patents.google.com/?q=D01D5\%2f0076.

[2] Z.-M. Huang, Y. Z. Zhang, M. Kotaki, S. Ramakrishna, A review on polymer nanofibers by electrospinning and their applications in nanocomposites, Composites Science and Technology 63 (15) (2003) 2223–2253. doi:10.1016/S0266-3538(03)00178-7.

[3] D. H. Reneker, A. L. Yarin, Electrospinning jets and polymer nanofibers, Polymer 49 (10) (2008) 2387–2425. doi:10.1016/J.POLYMER.2008.02.002.

[4] J. D. Schiffman, C. L. Schauer, A Review: Electrospinning of Biopolymer Nanofibers and their Applications, Polymer Reviews 48 (2) (2008) 317–352. doi:10.1080/15583720802022182.

[5] Q. Li, Chapter 7: Liquid Crystal-Functionalized Nano- and Microfibers Produced by Electrospinning - Liquid Crystals Beyond Displays: Chemistry, Physics, and Applications, John Wiley & Sons, 2012. doi:9781118078617.

[6] R. Kessick, J. Fenn, G. Tepper, The use of AC potentials in electrospraying and electrospinning processes, Polymer 45 (9) (2004) 2981–2984. doi:10.1016/j.polymer.2004.02.056.

[7] S. Sarkar, S. Deevi, G. Tepper, Biased AC electrospinning of aligned polymer nanofibers, Macromolecular Rapid Communications 28 (9) (2007) 1034–1039. doi:10.1002/marc.200700053.

[8] C. Attila, R. Demuth, null Balazs, G. Verreck, J. Mensch, G. Marosi, Z. Nagy, null Kristof, Alternating current electrospinning for preparation of fibrous drug delivery systems, International Journal of Pharmaceutics 495 (1) (2015) 75–80, Alternating current electrospinning,Dissolution enhancement,Electrospinning,Poorly water-soluble

drugs. Solid dispersion. doi:10.1016/j.ijpharm.2015.08.069.
URL http://dx.doi.org/10.1016/j.ijpharm.2015.08.069

[9] T. D. Brown, P. D. Dalton, D. W. Hutmacher, Melt electrospinning today: An opportune time for an emerging polymer process, Progress in Polymer Science 56 (2016) 116–166. doi:10.1016/j.progpolymsci.2016.01.001.

[10] Z. K. Nagy, A. Balogh, G. Drávavölgyi, J. Ferguson, H. Pataki, B. Vajna, G. Marosi, Solvent-Free Melt Electrospinning for Preparation of Fast Dissolving Drug Delivery System and Comparison with Solvent-Based Electrospun and Melt Extruded Systems, Journal of Pharmaceutical Sciences 102 (2) (2013) 508–517. doi:10.1002/jps.23374.

[11] A. Balogh, G. Drávavölgyi, K. Faragó, A. Farkas, T. Vigh, P. L. Sóti, I. Wagner, J. Madarász, H. Pataki, G. Marosi, Z. K. Nagy, Plasticized drug-loaded melt electrospun polymer mats: Characterization, thermal degradation, and release kinetics, Journal of Pharmaceutical Sciences 103 (4) (2014) 1278–1287. doi:10.1002/jps.23904.

[12] H. Lian, Z. Meng, Melt electrospinning vs. solution electrospinning: A comparative study of drug-loaded poly (ε-caprolactone) fibres, Materials Science and Engineering C 74 (2017) 117–123. doi:10.1016/j.msec.2017.02.024.

[13] G. Hochleitner, M. Kessler, M. Schmitz, A. R. Boccaccini, J. Teβmar, J. Groll, Melt electrospinning writing of defined scaffolds using polylactide-poly(ethylene glycol) blends with 45S5 bioactive glass particles, Materials Letters 205 (2017) 257–260. doi:10.1016/j.matlet.2017.06.096.

[14] †Jesse T. McCann, ‡, M. Marquez, †Younan Xia*, Melt Coaxial Electrospinning: A Versatile Method for the Encapsulation of Solid Materials and Fabrication of Phase Change Nanofibers (2006). doi:10.1021/NL0620839.

[15] K. Sarkar, C. Gomez, S. Zambrano, M. Ramirez, E. D. Hoyos, H. Vasquez, K. Lozano, Electrospinning to Forcespinning^{TM}, Materials Today 13 (11) (2010) 12–14. doi:10.1016/S1369-7021(10)70199-1.

[16] S. Mahalingam, M. Edirisinghe, Forming of polymer nanofibers by a pressurised gyration process, Macromolecular Rapid Communications 34 (14) (2013) 1134–1139. doi:10.1002/marc.201300339.

[17] M. R. Badrossamay, H. A. McIlwee, J. A. Goss, K. K. Parker, Nanofiber Assembly by Rotary Jet-Spinning, Nano Letters 10 (6) (2010) 2257–2261. doi:10.1021/nl101355x.

[18] N. E. Zander, Formation of melt and solution spun polycaprolactone fibers by centrifugal spinning, Journal of Applied Polymer Science 132 (2) (2015) 1–9. doi:10.1002/app.41269.

[19] L. A. Mary, T. Senthilram, S. Suganya, L. Nagarajan, J. Venugopal, S. Ramakrishna, V. R. G. Dev, Centrifugal spun ultrafine fibrous web as a potential drug delivery vehicle, Express Polymer Letters 7 (3) (2012) 238–248. doi:10.3144/expresspolymlett.2013.22.

[20] X. Zhang, Y. Lu, Centrifugal spinning: An alternative approach to fabricate nanofibers at high speed and low cost, Polymer Reviews 54 (4) (2014) 677–701. doi:10.1080/15583724.2014.935858.

[21] O. O. Dosunmu, G. G. Chase, W. Kataphinan, D. H. Reneker, Electrospinning of polymer nanofibres from multiple jets on a porous tubular surface, Nanotechnology 17 (4) (2006) 1123–1127. doi:10.1088/0957-4484/17/4/046.

[22] M. Kancheva, A. Toncheva, N. Manolova, I. Rashkov, Advanced centrifugal electrospinning setup, Materials Letters 136 (2014) 150–152. doi:10.1016/j.matlet.2014.08.045.

[23] A. E. Erickson, D. Edmondson, F. C. Chang, D. Wood, A. Gong, S. L. Levengood, M. Zhang, High-throughput and high-yield fabrication of uniaxially-aligned chitosan-based nanofibers by centrifugal electrospinning, Carbohydrate Polymers 134 (2015) 467–474. doi:10.1016/j.carbpol.2015.07.097.

[24] C. C. Liao, C. C. Wang, K. C. Shih, C. Y. Chen, Electrospinning fabrication of partially crystalline bisphenol A polycarbonate nanofibers: Effects on conformation, crystallinity, and mechanical properties, European Polymer Journal 47 (5) (2011) 911–924. doi:10.1016/j.eurpolymj.2011.01.006.

[25] D. Edmondson, A. Cooper, S. Jana, D. Wood, M. Zhang, Centrifugal electrospinning of highly aligned polymer nanofibers over a large area, Journal of Materials Chemistry 22 (35) (2012) 18646. doi:10.1039/c2jm33877g.

[26] M. A. Souza, K. Y. Sakamoto, L. H. C. Mattoso, Release of the diclofenac sodium by nanofibers of poly(3-hydroxybutyrate- co -3-hydroxyvalerate) obtained from electrospinning and solution blow spinning, Journal of Nanomaterials 2014 (2014). doi:10.1155/2014/129035.

[27] A. Cisquella-Serra, M. Magnani, Álvaro Gual-Mosegui, S. Holmberg, M. Madou, M. Gamero-Castaño, Study of the electrostatic jet initiation in near-field electrospinning, Journal of Colloid and Interface Science 543 (2019) 106–113. doi:10.1016/J.JCIS.2019.02.041.

[28] S. K. Nataraj, K. S. Yang, T. M. Aminabhavi, Polyacrylonitrile-based nanofibers—A state-of-the-art review, Progress in Polymer Science 37 (3) (2012) 487–513. doi:10.1016/J.PROGPOLYMSCI.2011.07.001.

[29] G. S. Bisht, G. Canton, A. Mirsepassi, L. Kulinsky, S. Oh, D. Dunn-Rankin, M. J. Madou, Controlled Continuous Patterning of Polymeric Nanofibers on Three-Dimensional Substrates Using Low-Voltage

Near-Field Electrospinning, Nano Letters 11 (4) (2011) 1831–1837. doi:10.1021/nl2006164.

[30] C. Chang, K. Limkrailassiri, L. Lin, Continuous near-field electrospinning for large area deposition of orderly nanofiber patterns, Appl Phys Lett (2008) 3doi:10.1063/1.2975834.

[31] J. Kim, B. Maeng, J. Park, Characterization of 3D electrospinning on inkjet printed conductive pattern on paper, Micro and Nano Systems Letters 6 (1) (2018) 12. doi:10.1186/s40486-018-0074-1.

[32] A. Gupta, A. M. Seifalian, Z. Ahmad, M. J. Edirisinghe, M. C. Winslet, Novel Electrohydrodynamic Printing of Nanocomposite Biopolymer Scaffolds, Journal of BIOACTIVE AND COMPATIBLE POLYMERS 22 (2007). doi:10.1177/0883911507078268.

[33] H. Wang, S. Huang, F. Liang, P. Wu, M. Li, S. Lin, X. Chen, Research on Multinozzle Near-Field Electrospinning Patterned Deposition, Journal of Nanomaterials 2015 (2015) 1–8. doi:10.1155/2015/529138.

[34] Z. Wang, X. Chen, J. Zeng, F. Liang, P. Wu, H. Wang, Controllable deposition distance of aligned pattern via dual-nozzle near-field electrospinning, AIP Advances 7 (3) (2017) 035310. doi:10.1063/1.4974936.

[35] Z. Wang, X. Chen, J. Zhang, Y.-J. Lin, K. Li, J. Zeng, P. Wu, Y. He, Y. Li, H. Wang, Fabrication and evaluation of controllable deposition distance for aligned pattern by multi-nozzle near-field electrospinning, AIP Advances 8 (7) (2018) 075111. doi:10.1063/1.5032082.

[36] Y. Huang, Y. Duan, Y. Ding, N. Bu, Y. Pan, N. Lu, Z. Yin, Versatile, kinetically controlled, high precision electrohydrodynamic writing of micro/nanofibers, Scientific Reports 4 (1) (2015) 5949. doi:10.1038/srep05949.

[37] J.-Y. Zheng, H.-Y. Liu, X. Wang, Y. Zhao, W.-W. Huang, G.-F. Zheng, D.-H. Sun, Electrohydrodynamic Direct-Write Orderly Micro/Nanofibrous Structure on Flexible Insulating Substrate, Journal of Nanomaterials 2014 (2014) 1–7. doi:10.1155/2014/708186.

[38] N. Bu, Y. Huang, X. Wang, Z. Yin, Materials and Manufacturing Processes Continuously Tunable and Oriented Nanofiber Direct-Written by Mechano-Electrospinning Continuously Tunable and Oriented Nanofiber Direct-Written by Mechano-Electrospinning (2012). doi:10.1080/10426914.2012.700145.

[39] A. R. Nagle, C. D. Fay, Z. Xie, G. G. Wallace, X. Wang, M. J. Higgins, A direct 3D suspension near-field electrospinning technique for the fabrication of polymer nanoarrays, Nanotechnology 30 (19) (2019) 195301. doi:10.1088/1361-6528/ab011b.

[40] Y. Duan, Y. Ding, Z. Xu, Y. Huang, Z. Yin, Helix Electrohydrodynamic Printing of Highly Aligned Serpentine Micro/Nanofibers., Polymers 9 (9) (sep 2017). doi:10.3390/polym9090434.

[41] C. Song, J. A. Rogers, J.-M. Kim, H. Ahn, Patterned polydiacetylene-embedded polystyrene nanofibers based on electrohydrodynamic jet printing, Macromolecular Research 23 (1) (2015) 118–123. doi:10.1007/s13233-015-3024-2.

[42] J. Jiang, X. Wang, W. Li, J. Liu, Y. Liu, G. Zheng, J. Jiang, X. Wang, W. Li, J. Liu, Y. Liu, G. Zheng, Electrohydrodynamic Direct-Writing Micropatterns with Assisted Airflow, Micromachines 9 (9) (2018) 456. doi:10.3390/mi9090456.

[43] S. Coppola, V. Vespini, G. Nasti, O. Gennari, S. Grilli, M. Ventre, M. Iannone, P. A. Netti, P. Ferraro, Tethered Pyro-Electrohydrodynamic Spinning for Patterning Well-Ordered Structures at Micro-and Nanoscale, Chem. Mater 26 (2014) 3360. doi:10.1021/cm501265j.

[44] J. Zheng, Y. Z. Long, B. Sun, Z. H. Zhang, F. Shao, H. D. Zhang, Z. M. Zhang, J. Y. Huang, Polymer nanofibers prepared by low-voltage near-field electrospinning, Chinese Physics B 21 (4) (2012) 1–6. doi:10.1088/1674-1056/21/4/048102.

[45] C.-T. Pan, C.-K. Yen, Z.-H. Liu, H.-W. Li, S.-W. Kuo, Y.-S. Lu, Y.-C. Lai, Poly(γ-benzyl α, l-glutamate) in Cylindrical Near-Field Electrospinning Fabrication and Analysis of Piezoelectric Fibers (2014).

[46] C.-T. Pan, C.-K. Yen, S.-Y. Wang, Y.-C. Lai, L. Lin, J. C. Huang, S.-W. Kuo, Near-field electrospinning enhances the energy harvesting of hollow PVDF piezoelectric fibers, RSC Advances 5 (103) (2015) 85073–85081. doi:10.1039/C5RA16604G.

[47] S. Chakraborty, I.-C. Liao, A. Adler, K. W. Leong, Electrohydrodynamics: A facile technique to fabricate drug delivery systems, Advanced Drug Delivery Reviews 61 (12) (2009) 1043–1054. doi:10.1016/j.addr.2009.07.013.

[48] K. A. G. Katsogiannis, G. T. Vladisavljević, S. Georgiadou, Porous electrospun polycaprolactone (PCL) fibres by phase separation, European Polymer Journal 69 (2015) 284–295. doi:10.1016/j.eurpolymj.2015.01.028.

[49] J. Kameoka, H. G. Craighead, Fabrication of oriented polymeric nanofibers on planar surfaces by electrospinning, Applied Physics Letters 83 (2) (2003) 371–373. doi:10.1063/1.1592638.

[50] D. Sun, C. Chang, S. Li, L. Lin, Near-Field Electrospinning (2006). doi:10.1021/nl0602701.

[51] N. Xue, X. Li, C. Bertulli, Z. Li, A. Patharagulpong, A. Sadok, Y. Y. S. Huang, Rapid Patterning of 1-D Collagenous Topography as an ECM Protein Fibril Platform for Image Cytometry, PLoS ONE 9 (4) (2014) e93590. doi:10.1371/journal.pone.0093590.

[52] D. D. Camillo, V. Fasano, F. Ruggieri, S. Santucci,

L. Lozzi, A. Camposeo, D. Pisignano, Near-field electrospinning of conjugated polymer light-emitting nanofibers, Nanoscale 5 (2013) 11637–11642. doi:10.1039/C3NR03094F.

[53] Q. Xiang, Y.-M. Ma, D.-G. Yu, M. Jin, G. R. Williams, Electrospinning using a Teflon-coated spinneret, Applied Surface Science 284 (2013) 889–893. doi:10.1016/j.apsusc.2013.08.030.

[54] Q. Wang, D. G. Yu, S. Y. Zhou, C. Li, M. Zhao, Electrospun amorphous medicated nanocomposites fabricated using a Teflon-based concentric spinneret, E-Polymers 18 (1) (2018) 3–11. doi:10.1515/epoly-2017-0110.

[55] S.-Y. Min, T.-S. Kim, B. J. Kim, H. Cho, Y.-Y. Noh, H. Yang, J. H. Cho, T.-W. Lee, Large-scale organic nanowire lithography and electronics, Nature Communications 4 (1) (2013) 1773. doi:10.1038/ncomms2785.

[56] J. Xu, M. Abecassis, Z. Zhang, P. Guo, J. Huang, K. Ehmann, J. Cao, Accuracy Improvement of Nano-fiber Deposition by Near-Field Electrospinning, International Workshop on Microfactories IWMF2014 (9th) (2014).

[57] Z. H. Liu, C. T. Pan, L. W. Lin, J. C. Huang, Z. Y. Ou, Direct-write PVDF nonwoven fiber fabric energy harvesters via the hollow cylindrical near-field electrospinning process (2014) 25003–25014doi:10.1088/0964-1726/23/2/025003.

[58] W. S. Choi, G. H. Kim, J. H. Shin, G. Lim, T. An, Electrospinning onto Insulating Substrates by Controlling Surface Wettability and Humidity, Nanoscale Research Letters 12 (2017). doi:10.1186/s11671-017-2380-6.

[59] D. D. Camillo, V. Fasano, F. Ruggieri, S. Santucci, L. Lozzi, A. Camposeo, D. Pisignano, Near-field electrospinning of conjugated polymer light-emitting nanofibers, Nanoscale 5 (2013) 11637–11642. doi:10.1039/C3NR03094F.

[60] G. Zheng, W. Li, X. Wang, D. Wu, D. Sun, L. Lin, Precision deposition of a nanofibre by near-field electrospinning, Journal of Physics D: Applied Physics 43 (41) (2010) 415501. doi:10.1088/0022-3727/43/41/415501.

[61] D. Shin, J. Kim, J. Chang, Experimental study on jet impact speed in near-field electrospinning for precise patterning of nanofiber, Journal of Manufacturing Processes 36 (2018) 231–237. doi:10.1016/J.JMAPRO.2018.10.011.